

Analyzing the Strength of Fractured and Anisotropic Rock Masses: A Comparative Study of Synthetic Models and Empirical Approaches

Pedro P. Cacciari *Polytechnique Montréal, Montréal, Canada*

Lucas T. Figueiredo *Anglo American, Belo Horizonte, Brazil*

Alexandre Gontijo, Guilherme Ribas *MecRoc, Belo Horizonte, Brazil*

Abstract

This article compares the synthetic rock mass (SRM) modeling approach with empirical methods used to obtain the equivalent strength of rock masses. In the first case, a parametric study utilized Discrete Fracture Networks (DFN) and a lattice-based Discrete Element Method (DEM) to create SRM models of a hypothetical rock mass with a single random joint set. The results indicate a poor agreement between SRM and empirical methods for predicting the uniaxial compressive strength of rock masses. The SRM method appears to be more sensitive to changes in intensity and persistence. In contrast, empirical-based methods may underestimate this parameter by employing ineffective measures (e.g., RQD, spacing, and unspecific discontinuity size measurements). In the second case, the SRM method is applied to a fractured and foliated rock mass from an open pit mine. The results show that the rock mass remains anisotropic after including DFNs of two joint sets in the numerical model, highlighting the importance of using SRM modeling to verify if the rock mass can be considered an equivalent isotropic medium. They also indicate that the empirical method can both underestimate and overestimate rock mass strength, depending on the foliation dip and the method used to address anisotropy within the empirical approach.

1 Introduction

The synthetic rock mass (SRM) modeling approach is a state-of-the-art technique that combines discrete fracture networks (DFN) and discrete element method (DEM) to create numerical models of discontinuous rock masses (Ivars et al. 2011). This approach holds tremendous potential for studying the mechanical behavior of rock masses at any scale. For anisotropic rocks, (Sainsbury and Sainsbury 2017) have emphasized the importance of providing ubiquitous-joint constitutive properties to anisotropic rock masses by calibrating continuum models with results obtained from SRM simulations using the 3D distinct element method. Similar approaches have been adopted in practical cases for stability analysis of large open pits (Koegelenberg et al. 2019; Bester et al. 2021).

Point your camera for the QR Code on the side and save the event on your calendar.





April 14 to 19, 2024 

Fundação Dom Cabral 
Nova Lima, Minas Gerais, Brazil

The lattice-spring DEM (LS-DEM) method offers a practical alternative to particle-based methods, as it simplifies the model to a random assembly of point-mass particles (nodes) interconnected by massless springs in three-dimensional space (Cundall 2011). The simple formulation of LS-DEM makes it much more efficient than particle-based methods without sacrificing the capability to represent the brittle failure of rock bridges between fractures. However, LS-DEM is limited to small-strain problems, as particle positions are not updated over time.

The most commonly employed methods for estimating the mechanical properties of rock masses rely on empirical correlations based on rock mass classification systems, such as the Geological Strength Index (GSI) and the Rock Mass Rating (RMR). While both SRM-based and empirical methods can be used to assess the equivalent strength of rock masses, there are several factors that can lead to disparities between these approaches. Generally, empirical methods rely on simplified descriptions of joint geometrical parameters, using mean spacing and Rock Quality Designation (RQD) to represent the degree of fracturing in rock masses. Some of these empirical methods either assign a minor role to joint persistence or do not consider it at all. In contrast, in DFN-based SRM models, discontinuity geometrical parameters, such as orientation, frequency, intensity, and size, are often defined in detail and represented using probability distributions derived from field mapping (Cacciari and Futai, 2021 and 2022). However, SRM models rely on the calibration of several micro-parameters and, as probabilistic models based on random variables, they yield different results for each DFN run. Consequently, it is essential to verify and discuss the alignment between the methods based on Synthetic Rock Mass (SRM) and empirical approaches when estimating the strength of rock masses within the field of rock mechanics.

This paper presents two different cases that highlight the discrepancies between rock mass strength obtained by SRM and empirical methods. In the first case, a parametric study utilized DFN and a lattice-based DEM method to create SRM models of a hypothetical rock mass. A series of uniaxial compression tests were conducted with the SRM models, varying the discontinuity volumetric intensity and the size of a single joint set with random orientation to avoid any strength anisotropy in the models. The results indicate a poor agreement between SRM and empirical methods for predicting the uniaxial compressive strength of rock masses. The SRM method appears to be more sensitive to changes in intensity and persistence. In contrast, empirical-based methods may underestimate this parameter by employing ineffective measures (e.g., RQD, spacing, and unspecific discontinuity size measurements) and assigning low ratings to critical parameters that can influence the mechanical behavior of rock masses under unconfined or low-confining stress conditions. In the second case, the SRM method is applied to a fractured and foliated rock mass from an open-pit mine. In this case, SRM models were created by integrating UAV geological mapping and DFN modeling. The SRM models were rotated about the foliation strike to assess the influence of foliation and fractures on the strength anisotropy of the rock mass. The SRM results indicate that the empirical method can both underestimate and overestimate rock mass strength, depending on the foliation dip and the method used to address anisotropy with the empirical approach.

Point your camera for the QR Code on the side and save the event on your calendar.



realization



organization



2 Comparison between SRM and empirical methods for a single random joint set

Empirical methods are used to obtain the equivalent mechanical parameters of rock masses. In most cases, these methods assume that fractured rock mass behave as an isotropic media after a certain scale and fracturing degree. For the Geological Strength Index, for example, the authors highlight that system is based upon the assumption that the rock mass contains a sufficient number of “randomly” oriented discontinuities such that it behaves as an isotropic mass (Marinos et al., 2005).

To compare SRM models and empirical methods, a single set of randomly oriented discontinuities (Fisher $K=1$) was used to represent a hypothetical rock mass. Table 1 summarizes the parameters used in these analyses. Figure 1 shows the dimensions of the model. 10 DFN were simulated for each combination of volumetric intensity (P_{32}) and mean discontinuity diameter (μ_D) in Table 1. A virtual scanline (see Figure 1), placed in the middle of the DFN domain, was used to calculate the linear frequency (P_{10}) spacing ($1/P_{10}$) of each DFN simulation.

Table 1. Properties of the DFNs used by Cacciari and Futai (2022).

Random joint set	
Volumetric intensity, P_{32} (m ⁻¹)	0.25; 0.5; 1.5; 2.5; 3.5; 4.5
Orientation distribution	Fisher
Dip/Dip direction	Random (Fisher $k=1$)
Size distribution	Log-normal
Coefficient of variation of disk diameters, CoV	0.5
Mean disk diameters, μ_D (m)	0.5; 0.8; 1.2; 2.0; 4.0

Point your camera for the QR Code on the side and save the event on your calendar.



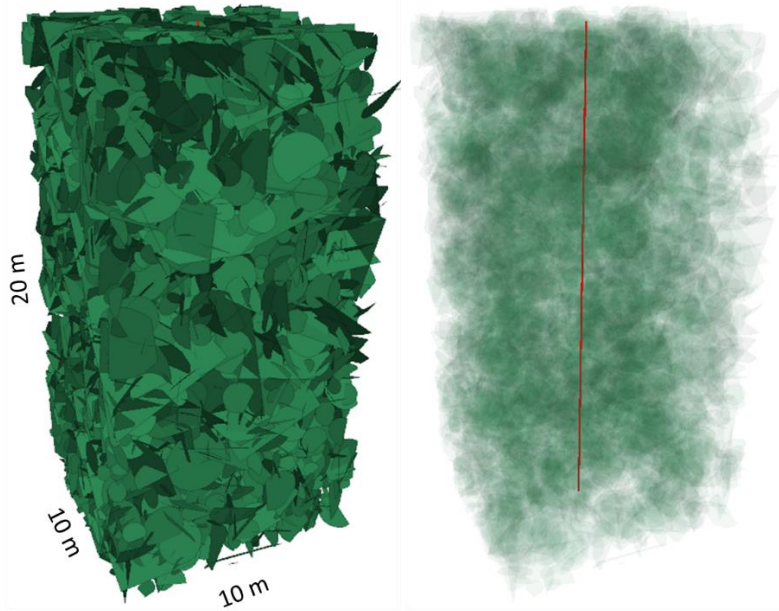


Figure 1. DFN model and vertical the scanline used to compute P_{10} of each simulation.

Equation 1 (Priest, 1995) was used to calculate the theoretical rock quality designation (TRQD) with the threshold of $t=0.1$ m:

$$TRQD_{0.1} = 100e^{-P_{10}t}(1 + P_{10}0.1) \quad (1)$$

The values of TRQD, joint spacing ($1/P_{10}$) and persistence (e.g., μ_D) were used to calculate the respective rock mass ratings (RMR_{89}) for each $P_{32}-\mu_D$ combination in Table 1.

Cacciari and Futai (2022) used the same parameters and same DFN domain sizes to investigate the individual effects of P_{32} and μ_D (intensity and persistence) on the mechanical behavior of a hypothetical rock mass with a single joint set of random orientation. In this case, the SRMTools software (Itasca Consulting Group) was used to run the uniaxial compression tests of rock masses. This three-dimensional modeling software is based on LS-DEM that handles discontinuities and new fractures in the same way as other discrete methods (Cacciari and Futai, 2022).

Simplified properties were adopted to represent the mechanical behavior of the intact rock and discontinuities. For the intact rock, the uniaxial compressive strength (UCS), tensile strength, Young's Modulus, and Poisson's ratio adopted were 100 MPa, 7.0 MPa, 50 GPa, and 0.3,

Point your camera for the QR Code on the side and save the event on your calendar.



respectively. The UCS of the intact rock was properly calibrated to match the adopted value using the flat joint model available on the software. For the discontinuities, the standard Mohr-Coulomb envelope was used with a friction coefficient of 0.5 (null cohesion and tensile strength), normal stiffness, and shear stiffness of 30 and 3 GPa/m, respectively.

Figure 2a shows the expected linear correlation between P_{32} and P_{10} obtained for each $P_{32}-\mu_D$ combination in Table 1. Figure 2b shows the $TRQD_{0.1}$ calculated for each P_{10} (Equation 1), indicating a small variation of TRQD for a wide range of volumetric intensity. Figure 3 shows the final RMR_{89} calculated with the TRQD, μ_D , and spacings ($1/P_{10}$) obtained from DFN analysis. The other parameters required to calculate RMR_{89} were fixed as follows:

- Uniaxial compressive strength: 100 MPa adopted as intact rock strength and used to run the LS-DEM models. Rating=10.
- Joint conditions (except for persistence): Aperture + roughness + infilling + weathering. Rating=15. The μ_D values in Table 1 were used to calculate the persistence ratings (from 1 to 6) for each $P_{32}-\mu_D$ combination.
- Ground water: Completely dry. Rating=15.

These parameters provide a fixed initial RMR_{89} of 40. For each $P_{32}-\mu_D$ combination, the respective ratings from TRQD, μ_D (persistence conditions), and spacings ($1/P_{10}$) were added to the initial RMR_{89} value.

Figure 3 shows examples of SRM results (from Cacciari and Futai 2022) using the DFN-LS-DEM method. Figures 4 show the comparison between strength ratios, defined by the uniaxial compressive strength of the intact rock (UCS_i) divided by the uniaxial compressive strength of the rock mass (UCS_{rm}), obtained from SRM modeling (DFN-LS-DEM approach) and four different empirical equations listed in Table 2.



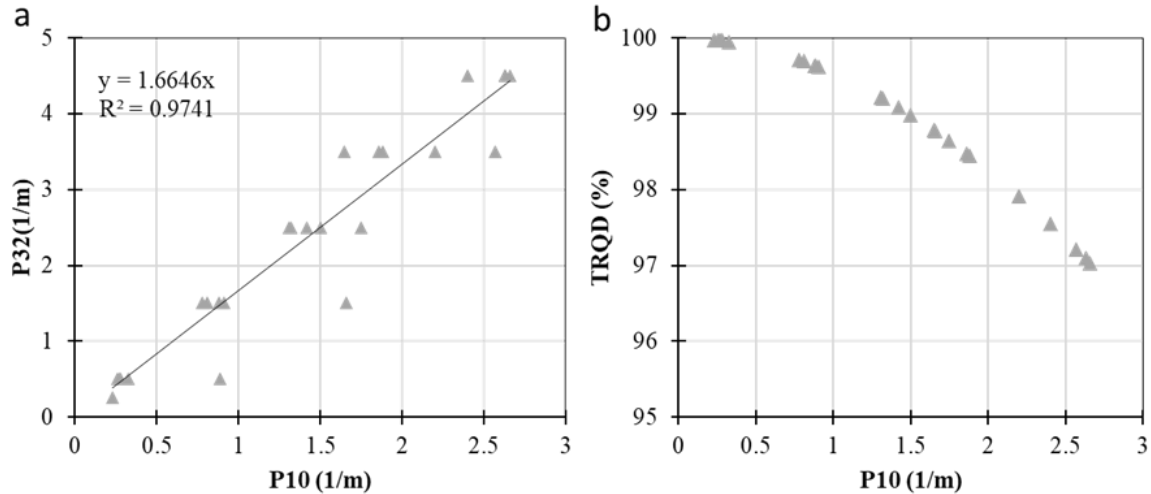


Figure 2. (a) P32 x P10 and (b) TRQD0.1 x P10.

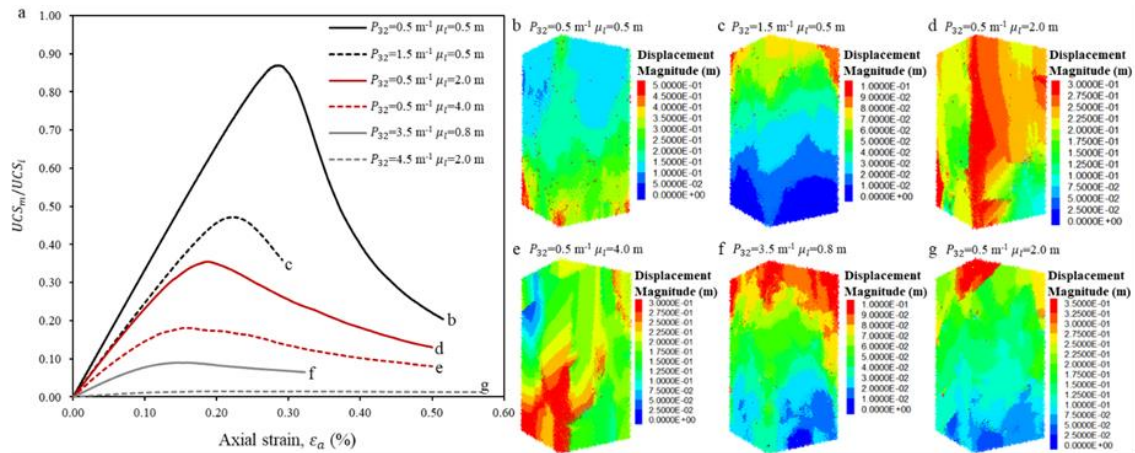


Figure 3. Examples of LS-DEM results (extracted from Cacciari and Futai 2022).

Table 2. Empirical correlations between UCS and RMR applied in this work.

Authors	Equation
Yudhbir et al. (1983)	$\sigma_{cm} = \sigma_{ci} e^{7.65 \left(\frac{RMR-100}{100} \right)}$
Ramamurthy (1986)	$\sigma_{cm} = \sigma_{ci} e^{\left(\frac{RMR-100}{18.75} \right)}$

Point your camera for the QR Code on the side and save the event on your calendar.



Kalamaras and Bieniawski (1995)

$$\sigma_{cm} = \sigma_{ci} e^{\left(\frac{RMR-100}{24}\right)}$$

$$\sigma_{cm} = \sigma_{ci} \times S^a$$

Hoek et al. (2002)

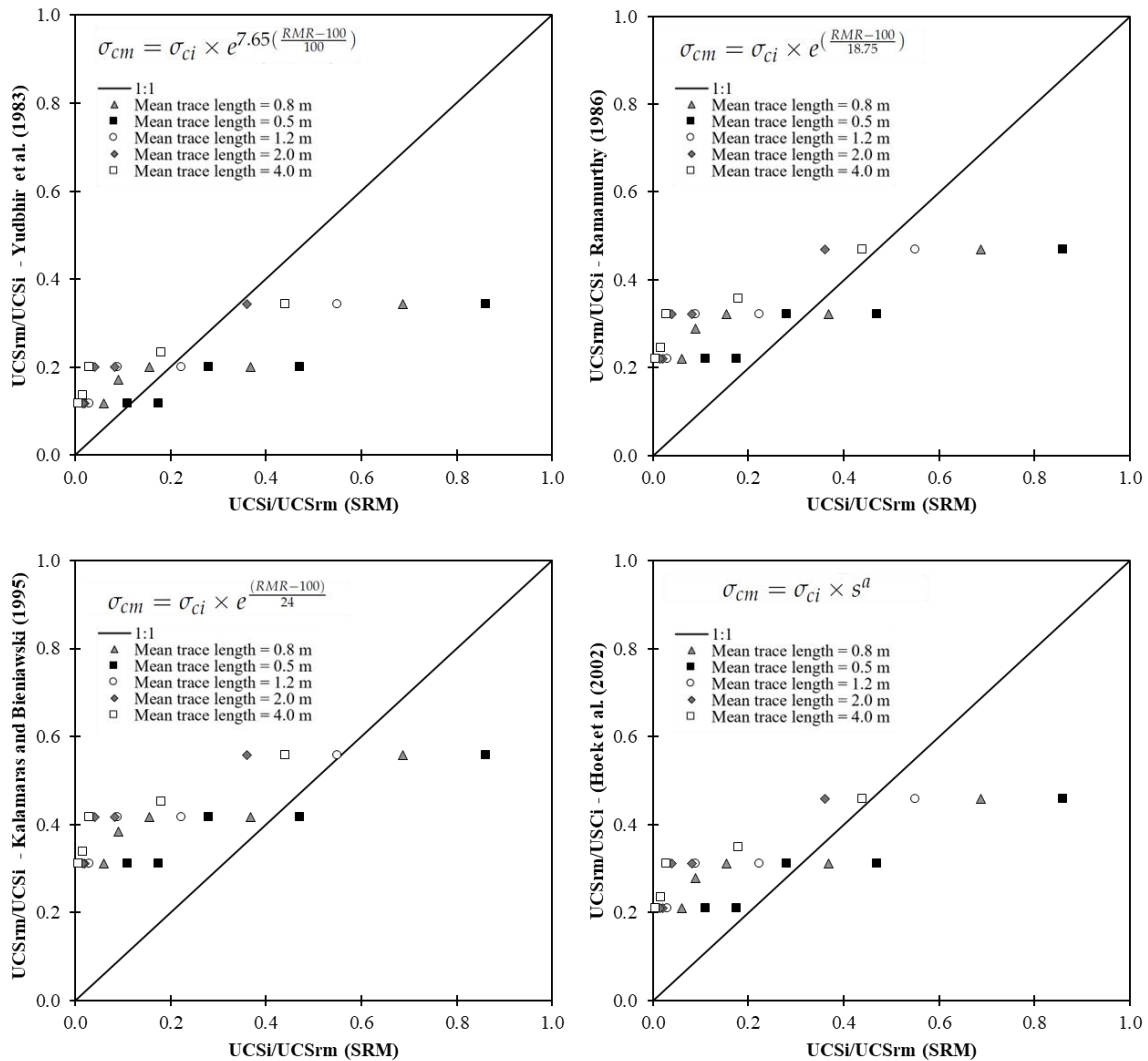


Figure 4. Comparison between UCSi/UCSrm obtained from SRM modeling (DFN-LS-DEM approach) and four different empirical equations listed in Table 2.

Point your camera for the QR Code on the side and save the event on your calendar.



Figure 4 shows a poor agreement between SRM and empirical methods. Overall, these results show that, for a rock mass composed by a single hard rock type ($UCS_i=100\text{MPa}$), joints tend to have moderate influence on the rock mass strength calculated by empirical methods. The minimum and maximum values of UCS_i/UCS_{rm} calculated by these methods vary between 0.15-0.30 and 0.35-0.55, respectively. In contrast, SRM models can result in UCS_i/UCS_{rm} from almost zero to 0.90, depending on joint size and intensity. These differences can be explained by three main reasons:

- The rating of joint persistence in RMR may not reflect the major role of joint size on the rock mass strength. It is important to note that other empirical methods do not take joint size into account.
- The number of non-persistent joint in the models does not change RQD substantially (see Figure 2b). The minimum value of 97% was found for a $P_{32}=4.5$. In this case, only spacing ($1/P_{10}$) is changing the RMR ratings related to fracturing degree.
- The fixed initial rating, based on parameters unrelated to joint geometry (e.g., 40), leads to a relatively high minimum strength value for UCS_{rm} when obtained through empirical methods. In other words, for large-spaced, non-persistent joints, the calculated strength values do not vary significantly. However, it is logical to assume that joints will always influence the mechanical behavior of rock masses, particularly under low or zero confining conditions.

3 SRM modelling of an anisotropic rock mass in an open pit mine

2.1 DFN modeling based on UAV mapping.

The Matrice 300 RTK drone, equipped with the Zenmuse P1 camera, was utilized to capture a high-resolution point cloud of a slope face from an important iron ore mine in Minas Gerais, Brazil. The images were taken from around 20 meters from the slope face, and a manual capture method was used to ensure a minimum of 70% overlap between the images. The acquired images were processed through photogrammetry using Agisoft Metashape software, resulting in the final point cloud depicted in Figure 5a. The point cloud density in the mapping area was carefully maintained to ensure a minimum density of approximately 2 points/cm².

P_{32} , calculated as the total discontinuity area by rock mass volume, is the most suitable parameter to quantify discontinuities within rock masses (Cacciari and Futai 2022). It includes both the 3D discontinuity density (number of discontinuities by the rock mass volume) and size and is independent of discontinuity orientation. Computational methods are necessary to estimate P_{32} of discontinuities within rock masses, as direct estimation from rock outcrops and boreholes is impossible. In this paper the following steps were used to model DFNs from geological mapping:

1. Select a region of the rock face and obtain a best-fit plane (Figure 5a and 5b). This geometry represents the virtual sampling plane (VSP). The VSP is also used as a convex sampling window



(Mauldon, 1998) to calculate the mean trace length (μ) and the standard deviation of trace lengths (σ) of joint sets.

2. Define the discontinuity size (disk diameters) and the orientation distribution (Fisher) by discontinuity analysis methods. The analytical solutions proposed by Zhang and Einstein (2000) were used to find the disk diameter distribution from trace lengths.
3. Transfer the VSP to the interior of the DFN domain. Run DFN simulations using the mapped P_{20} (number of fractures divided by the VSP area) as the joint density criterion (Figure 2b) and calculate the P_{32} . In this step, a Fish code was created to read STL files (VSP) and to use P_{20} as the density criterion.
4. Create a loop to run a specified number of DFN simulations (e.g., 10 runs) for each discontinuity set, changing the DFN domain size (the edge of the cubic DFN box in Figure 2b).
5. Verify the P_{32} variation with domain size and find the representative value.
6. Run the definitive DFN simulation using the mean P_{32} as the discontinuity intensity criterion. These DFNs (one for each fracture set) are used to create SRM models.

Step number 5 ensures that the P_{32} used is scale-independent, i.e., P_{32} does not change after a specific DFN domain size. This domain size represents the geometrical representative elementary volume (gREV). It also ensures that a representative value of volumetric intensity is used to run the DFN simulation and provide the discontinuity planes to the SRM models.

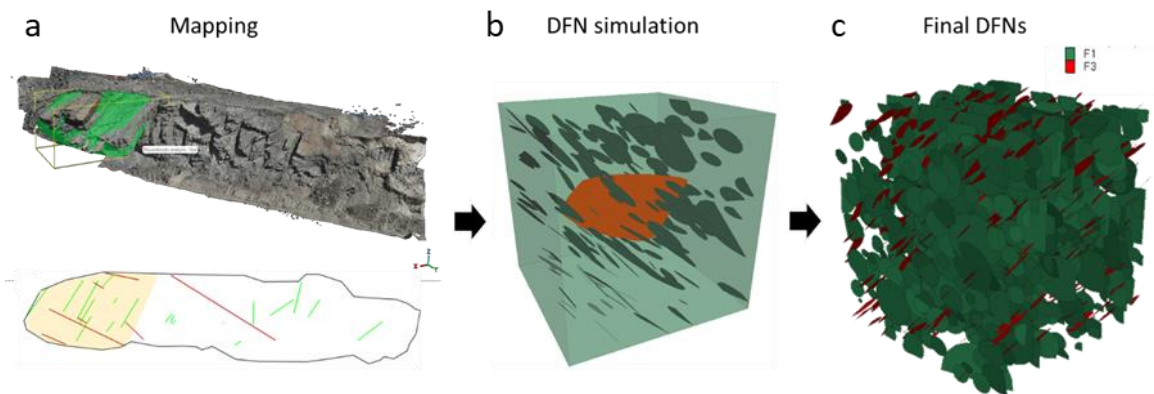


Figure 5. (a) UAV image and joint trace map with the VSP used to create DFNs. (b) One DFN run with the VSP inside the DFN domain. (c) Final DFNs from different joint sets after following steps 1-6.



2.2 SRM modeling

To calibrate the SRM model, the following parameters were used:

- Intact rock with foliation planes perpendicular to axial stress (from mining design database): Uniaxial Compressive Strength (UCSi) = 30 MPa, Young's Modulus (E) = 5 GPa, and Poisson's Ratio (ν) = 0.25.
- Foliation plane strength (from mining design database): JCS = 53 MPa, JRC = 2, and $\phi_r = 27$ degrees. Equivalent parameters for the Mohr-Coulomb envelope (cohesion $c_f = 0.01$ MPa and friction angle $\phi_f = 32$ degrees).

The intact rock is a semi-compact quartzite, with moderately altered by weathering. The SRM model with foliation planes perpendicular to the uniaxial stress were calibrated to match the intact rock parameters described above.

Figure 6a shows the results of intact rock simulations. All results are normalized by the maximum strength of intact rock (i.e., 30 MPa). This Figures shows a reasonable agreement between SRM results (for anisotropic intact rock) and the theoretical model (well-known Jaeger's model based on the dip of a plane of weakness). Figure 6b and 6c show the results of uniaxial and triaxial compression of rock mass, after in inclusion of the DFNs in Figure 5c. Numerical tests were conducted only for foliation with dip angles of 0, 40, and 55 degrees. These dips represent conditions perpendicular to the foliation, *in situ* (mean foliation dip mapped via UAV), and parallel to the foliation, respectively.

Figure 6b shows that the Hoek-Brown (HB) model with GSI=70, used at this mining site, is equivalent to SRM for a foliation dip of approximately 25 degrees. The empirical UCSi/UCS_{rm} ratio (from the HB model) yields a value of about 0.2, which falls approximately in the middle of the range, with the minimum being 0.03 and the maximum being 0.40, for UCSi/UCS_{rm} ratios obtained through SRM. Currently, in the mining design, UCS_{rm} is assumed to be 0 in the direction parallel to foliation planes, and the Barton Badis (BB) model is applied to represent rock mass strength in these conditions, as illustrated by the transition from HB (GSI=70) to UCS=0 in Figure 7a.

In Figure 6c, the first relevant observation is the similarity between the SRM results and the empirical model (HB) when the foliation is perpendicular to the axial stress and confinement exceeds 1 MPa. This result suggest that the discrepancies observed in Figure 4 for UCS may reduce in confined conditions. In contrast, there is a discrepancy between the numerical model (LS-DEM //55dg) and the BB envelope used to represent shear strength perpendicular to the foliation planes (MC from BB in Figure 6c). This difference occurs because the increase in confinement stresses causes interlocking of blocks in SRM models, consequently increasing the friction coefficient of the rock mass. As a result, the failure does not develop exclusively along a foliation plane.



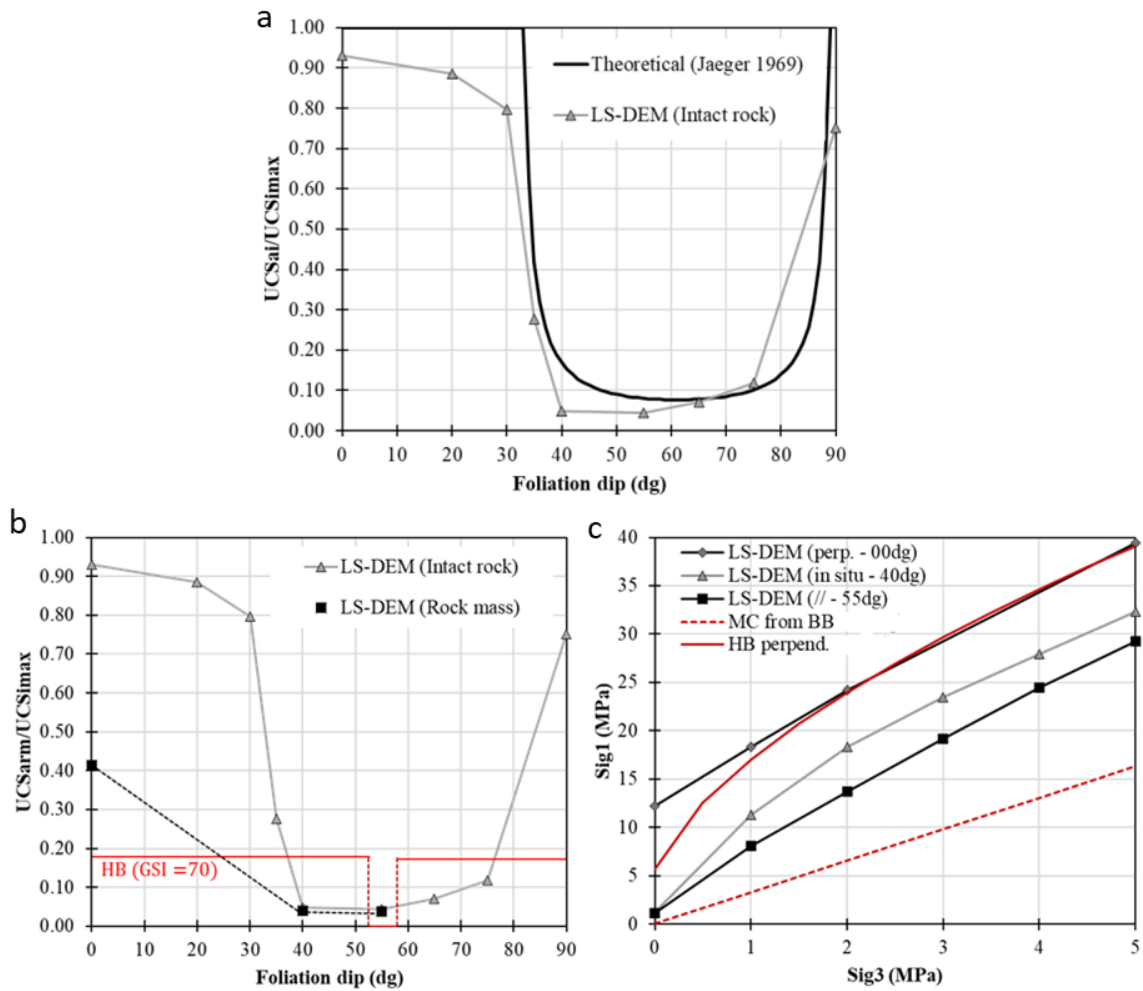


Figure 6. SRM results. (a) SRM vs. theoretical model by Jaeger (1969); (b) and (c) SRM vs. empirical method (HB with GSI=70) used in mining design at this location.

4 Conclusions

In conclusion, this study shows significant disparities in rock mass strength assessments between SRM and empirical methods. The first case, involving a hypothetical rock mass with a random joint set, reveals a notable incongruence in predicting the uniaxial compressive strength of rock masses. SRM displays heightened sensitivity to variations in intensity and persistence, while empirical



methods tend to underestimate this parameter by relying on less effective measures (e.g., RQD, spacing, and vague discontinuity size metrics) and assigning low ratings to crucial parameters that can govern the mechanical response of rock masses in unconfined or low-confining stress conditions. In the second case, where SRM is applied to a fractured and foliated rock mass from an open pit mine, the integration of UAV geological mapping and DFN modeling was used to build the SRM models. The results show that the rock mass remains anisotropic after including DFNs of two joint sets in the numerical model, highlighting the importance of using SRM modeling to verify if the rock mass can be considered an equivalent isotropic medium. The SRM outcomes suggest that the empirical approach can both underestimate and overestimate rock mass strength, depending on the foliation dip and the specific method employed to address anisotropy with the empirical approach.

5 References

- Ivars DM, Pierce ME, Darcel C, et al (2011) The synthetic rock mass approach for jointed rock mass modelling. *International Journal of Rock Mechanics and Mining Sciences* 48:219–244. <https://doi.org/10.1016/j.ijrmms.2010.11.014>
- Sainsbury BL, Sainsbury DP (2017) Practical Use of the Ubiquitous-Joint Constitutive Model for the Simulation of Anisotropic Rock Masses. *Rock Mech Rock Eng* 50:1507–1528. <https://doi.org/10.1007/s00603-017-1177-3>
- Koegelenberg C, Creus P, Bester M, et al (2019) A risk-based methodology to improve the definition of geotechnical sectors in slope design. *The Journal of the Southern African Institute of Mining and Metallurgy* 119:.. <https://doi.org/10.17159/2411>
- Bester M, Stacey TR, Russell T (2021) Synthetic Rock Mass Modelling and Geotechnical Mapping: An Open Pit Mine Case Study in Anisotropic Rock. *Int J Min Reclam Environ* 35:356–378. <https://doi.org/10.1080/17480930.2020.1834177>
- Cundall PA (2011) Lattice method for modeling brittle, jointed rock. In: *Continuum and Distinct Element Numerical Modeling in Geomechanics, Proceedings of the 2nd International FLAC/DEM Symposium, Melbourne, Australia*. pp 14–16
- Cacciari PP, Futai MM (2021) The Influence of Fresh and Weathered Rock Foliation on the Stability of the Monte Seco Tunnel. *Rock Mech Rock Eng* 54:537–558. <https://doi.org/10.1007/s00603-020-02292-z>
- Cacciari PP, Futai MM (2022) A Practical Method for Estimating the Volumetric Intensity of Non-persistent Discontinuities on Rock Exposures. *Rock Mech Rock Eng* 55:6063–6078. <https://doi.org/10.1007/s00603-022-02966-w>
- Marinos V, Marinos P, Hoek, E (2005) The geological strength index: applications and limitations. *Bull Eng Geol Environ* 64, 55–65. <https://doi.org/10.1007/s10064-004-0270-5>
- Priest SD (1993) *Discontinuity Analysis for Rock Engineering*. London: Chapman & Hall.
- Mauldon M (1998) Estimating Mean Fracture Trace Length and Density from Observations in Convex Windows. *Rock Mech Rock Eng* 31:201–216. <https://doi.org/10.1007/s006030050021>
- Zhang L, Einstein HH (2000) Estimating the intensity of rock discontinuities. *International Journal of Rock Mechanics and Mining Sciences* 37:819–837. [https://doi.org/10.1016/S1365-1609\(00\)00022-8](https://doi.org/10.1016/S1365-1609(00)00022-8)

